ELSEVIER

Journal of Biomechanics 36 (2003) 211–218

JOURNAL OF BIOMECHANICS

www.elsevier.com/locate/jbiomech
www.JBiomech.com

Hill muscle model errors during movement are greatest within the physiologically relevant range of motor unit firing rates

Eric J. Perreault*, Charles J. Heckman, Thomas G. Sandercock

Department of Physiology, Northwestern University Medical School, IL 60611, USA

Accepted 27 September 2002

Abstract

This study evaluated the accuracy of Hill-type muscle models during movement. Hill-type models are ubiquitous in biomechanical simulations. They are attractive because of their computational simplicity and close relation to commonly measured experimental variables, but there have been surprisingly few experimental validations of these models during functionally relevant conditions. Our hypothesis was that model errors during movement are largest at the low motor unit firing rates most relevant to normal movement conditions. This hypothesis was evaluated in the cat soleus muscle activated either by electrical stimulation at physiological rates or via the crossed-extension reflex (CXR) thereby obtaining normal patterns of motor unit recruitment and rate modulation. These activation paradigms were applied during continuous movements approximately matched to locomotor length changes. The resulting muscle force was modeled using a common Hill model incorporating independent activation, tetanic length–tension and tetanic force–velocity properties. Errors for this model were greatest for stimulation rates between approximately 10–20 Hz. Errors were especially large for muscles activated via the CXR, where most motor units appear to fire within this range. For large muscle excursions, such as those seen during normal locomotion, the errors for naturally activated muscle typically exceeded 50%, supporting our hypothesis and indicating that the Hill model is not appropriate for these conditions. Subsequent analysis suggested that model errors were due to the common Hill model's inability to account for the coupling between muscle activation and force–velocity properties that is most prevalent at the low motor unit firing rates relevant to normal activation.

Keywords: Muscle modeling; Hill model; Cat soleus

1. Introduction

Physiologically relevant models of muscle force generation are essential for creating realistic large-scale simulations to examine the role of muscle properties in controlling movement and posture. Hill-like models incorporating length–tension and force–velocity properties (Zajac, 1989; Winters, 1990) have become ubiquitous in such studies (Gerritsen et al., 1996; van der Helm, 2000). These models are attractive because of their computational simplicity and close relation to commonly measured experimental variables, but there have been surprisingly few experimental validations of Hill models during functionally relevant conditions. This study evaluated Hill-model performance using physiologically relevant neural inputs and muscle movements to provide bounds on the accuracy provided by such models and clues as to how these models should be improved to best simulate muscle behavior.

The most common Hill model incorporates the assumption that muscle force–velocity, length–tension and activation properties are mutually independent, an assumption known to be incorrect (Jewell and Wilkie, 1960; Rack and Westbury, 1969; Zahalak, 1986; Brown et al., 1999). As a consequence, such models do not capture many nonlinear muscle properties such as history-dependent effects (Edman et al., 1993; Morgan, 1994), length and movement-dependent activation (Caputo et al., 1994; Balnave and Allen, 1996), and yielding (Nichols and Houk, 1976). Therefore, numerous groups have modified the Hill model by incorporating these and other properties (Brown et al., 1996;

*Corresponding author. Departments of Biomedical Engineering and Physical Medicine and Rehabilitation, Northwestern University, 345 E. Superior Street, Room 1403, Chicago, IL 60611, USA. Tel.: +1-312-238-2226; fax: +1-312-238-2208.

E-mail address: e-perreault@northwestern.edu (E.J. Perreault).

0021-9290/03/$ - see front matter
PII: S0021-9290(02)00332-9

Meijer et al., 1998; Shue and Crago, 1998; Brown and Loeb, 2000). Many of these properties, though, have been demonstrated only under laboratory conditions using length and activation inputs that typically are not seen during functional behavior. Therefore, it is not yet clear whether such complex properties are required to predict muscle force responses during normal function.

A previous study in our laboratory (Sandercock and Heckman, 1997) evaluated the common Hill model during simulated locomotor activity in electrically stimulated cat soleus muscle and found model errors to be moderate during muscle contraction ($<10\%$). That study though, was restricted to electrically activated muscle and examined limited movements and stimulation patterns. The goal of the current work was to evaluate Hill model performance during more general conditions, including natural activation. Our specific hypothesis was that Hill model performance during movement is worst at the low motor unit firing rates most relevant to normal movement conditions.

2. Methods

Data were collected from the left hindlimb of 4 cats (2–3 kg). All procedures were approved by the Animal Care Committee at Northwestern University.

2.1. Surgical preparation

Initial surgical preparations were done under deep gaseous anesthesia (1.5–3.0% isoflurane), according to standard procedures in our lab (Sandercock and Heckman, 1997; Sandercock and Heckman, 2001). The soleus muscle was exposed by removing both heads of the gastrocnemius and the plantaris. The fine fascia surrounding the soleus was resected to fully expose the posterior surface of the muscle belly and its tendon. The soleus nerve was isolated and left in continuity. All other distal hindlimb nerves were cut, as were the nerves to the semitendinosus, semimembranosus, and biceps femoris. The distal soleus tendon was attached to a computer-controlled muscle puller via a calcaneal bone chip. Surgically exposed areas of the hindlimb were covered with a pool of mineral oil formed within the pulled-up skin flaps. A spinal laminectomy was performed from L4 to S1. Ipsilateral dorsal roots from L4 to S2 were transected to eliminate sensory feedback from the soleus. Contralateral dorsal roots were left intact, as were all ventral roots. A precollicular decerebration was performed by transecting the midbrain with an ophthalmic spatula and aspirating the entire forebrain. The calvarium was packed with saline-soaked cotton wool. The gaseous anesthesia was then discontinued and the animal was allowed to breathe room air. Radiant heat was used to maintain hindlimb and core temperatures within physiological limits. At the end of the experiment, animals were sacrificed with pentobarbital (100 mg/kg i.v.).

2.2. Protocols

Experiments were designed to evaluate the Hill model's ability to predict muscle force during movement. Random muscle length changes were used to obtain a broad measure of the model's capabilities. The nominal perturbation used in all experiments was matched to soleus length changes during unrestrained locomotion (Goslow et al., 1973). It had a length excursion of ± 8 mm and bandwidth ranging from 0 to 5 Hz, and was generated by lowpass filtering a normally distributed random waveform. Additional length excursions (± 1 and ± 4 mm) and bandwidths (2.5 and 10 Hz) were tested in selected animals to differentiate between the effects of muscle length and muscle velocity. All length perturbations were centered about an operating point 8 mm less than physiological maximum. Maximum physiological length (0 mm) corresponded to approximately 4 mm beyond the peak of the tetanic length–tension curve.

Muscle length was controlled by a computer-controlled muscle puller [AV-50; ADI, Alexandria, VA] operating as a position servo. This device had a stiffness of greater than 60 kN/m and a small signal position bandwidth of approximately 50 Hz. Muscle length was measured by an LVDT [500 DC-B; Shaevitz, Hampton, VA] attached to the puller shaft, and force was measured by a strain gage based transducer [Model 31(stiffness >2 MN/m); Sensotec, Columbus, OH] in series with the shaft. Force and position data were sampled at 1 kHz [MIO-16; National Instruments, Austin, TX] and saved to a hard disk.

Muscle force was controlled using either electrical stimulation or natural activation. Three animals were used for the electrical stimulation protocol and two for the natural activation protocol, with one of these used in both protocols. Electrical stimulation was applied either using fine stainless steel wires in the proximal and distal portions of the muscle belly or via hook electrodes on the ventral roots. Similar results were obtained with both methodologies. A stimulus intensity 50–100% above that required to elicit full recruitment produced repeatable and consistent forces during all trials. Stimulus trains had constant interpulse intervals (IPIs) and uniformly distributed random IPIs spanning the range from 0.01 s to twice the desired mean IPI (10, 20 and 30 Hz). Data were also collected at a 100 Hz constant stimulation rate in one animal. Stimulation and movement onsets coincided during electrical stimulation (see Figs. 2 and 4). Natural motor unit recruitment and rate modulation patterns were generated using the crossed-extension reflex (CXR) (Powers and Rymer,

1988). This was elicited using manual skin compression at the contralateral ankle and knee joints. Skin compression was adjusted to obtain a range of steady muscle forces, as observed by visual feedback.

The passive response to each perturbation was also measured. Passive responses were subtracted from those measured during muscle contractions to determine the active muscle response. Passive and active trials were separated by a 30 s rest period. To minimize fatigue, at least one minute separated all active trials.

2.3. Selection of crossed-extension trials

A potential problem with the CXR is that activation may vary during the course of measurement. A two-stage process was used to screen out trials with non-constant activation. All trials were initially screened by visual inspection and those with abrupt force changes were removed from further processing. An automated procedure was then used to detect more subtle activation changes. This procedure compared the force response during natural activation to those obtained at three levels of constant frequency electrical stimulation (10, 20, and 30 Hz), approximately spanning the range of normal firing rates for cat soleus (Cordo and Rymer, 1982). A sequential quadratic programming algorithm for constrained optimization [Matlab; The Mathworks, Natick, MA] was used to determine the weighting factors of the three constant stimulation trials to best match each CXR response (Fig. 5A—Results), an approach feasible for the soleus muscle, which contains only slow motor units (Burke et al., 1974). Optimization was performed over the first half of the movement, and validated over the second half. Only trials with RMS errors less than 20% during both the first and second half of the movements were selected for further processing. Using these limits, approximately 30% of the collected CXR trials were retained. Changing the acceptable errors limits to 10% and 30% did not affect the qualitative results, but did influence the number of trials available for analysis.

2.4. Hill-model estimation

The simplest possible Hill-type model, consisting of a contractile element in series with an elastic element, was simulated. The contractile element produces force according to Eq. (1), where $A(t)$ is the muscle activation function, $F_{LT}(L)$ is the normalized tetanic length–tension relationship, and $F_{FV}(V)$ is the normalized tetanic force–velocity relationship, measured at the muscle length corresponding to the peak of $F_{LT}(L)F_{LT}(L)$ and $F_{FV}(V)$ are normalized with respect to the maximal tetanic force (100 Hz) at the peak of the $L-T$ curve, F_{max}. Based upon previous results (Sandercock and Heckman, 1997), the series elastic element was

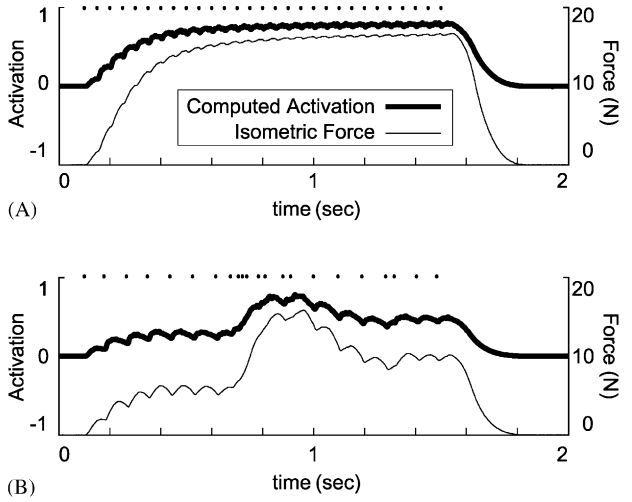

Fig. 1. The activation function for each stimulus protocol was computed directly using the isometrically measured muscle force response and the previously measured tetanic $F_{FV}(V)$ and $F_{LT}(L)$ curves. Isometric muscle length was set to the mean value used during the movement protocols (−8 mm). (A) Isometric force and computed activation function for 20 Hz continuous stimulation in a single animal. The dots at the top of the figure indicate actual stimulation times. (B) The same for 20 Hz random stimulation.

modeled as a piecewise exponential spring.

$$F_{CE} = F_{max}A(t)F_{LT}(L)F_{FV}(V). \quad (1)$$

The Hill model parameters describing $F_{LT}(L), F_{FV}(V)$ and the series elasticity were measured directly for each muscle, as described in detail previously (Sandercock and Heckman, 1997). In contrast, activation, $A(t)$, is difficult to define in Hill-type models. To avoid an arbitrary model, activation was defined using the experimental data. This was accomplished by applying each stimulation pattern during isometric conditions, measuring muscle force, and computing the activation that caused the Hill model to exactly recreate this force using the previously established $F_{LT}(L)$ and $F_{FV}(V)$ curves. Because the equations describing the Hill model are one-to one-functions, they can be inverted to solve for $A(t)$ (Fig. 1). Timing between isometric and movement trials was carefully controlled to avoid fatigue and potentiation.

The equations describing the Hill-type model were numerically integrated using a fourth order Runge–Kutta method (Press et al., 1986). The model inputs were muscle–tendon length, muscle–tendon velocity and $A(t)$. Errors between experimentally measured muscle force and that predicted by the Hill model were quantified using percent root mean square (RMS) values (Eq. (2)).

$$\text{Error} = \sqrt{\frac{\sum_N (F_{expt} - F_{Hill})^2}{\sum_N F_{expt}^2}} 100\%. \quad (2)$$

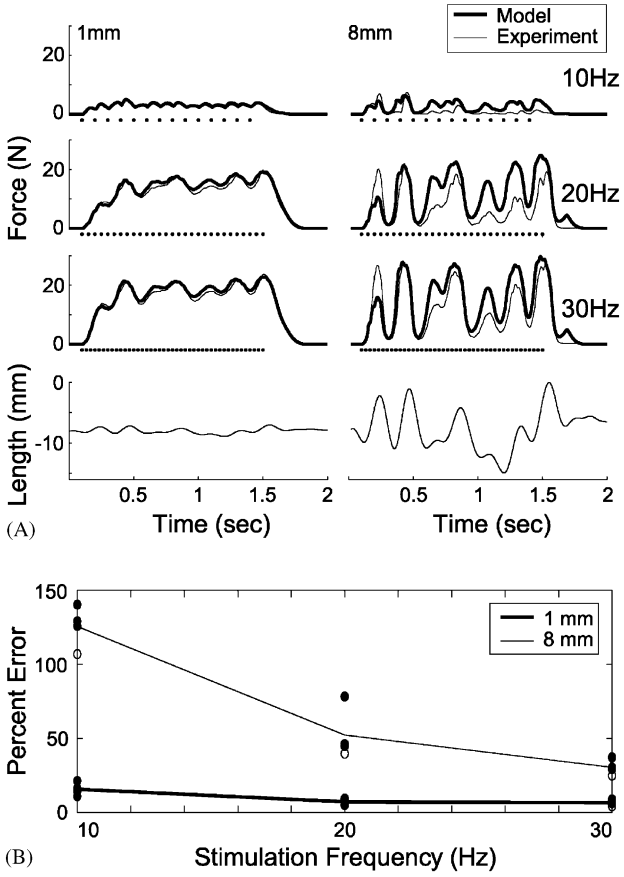

Fig. 2. Relative Hill-model errors during constant frequency stimulation increased with decreasing stimulation rate and increasing perturbation amplitude. (A) Typical data for one cat at constant stimulation rates of 10, 20, and 30 Hz. Results on the left are for ± 1 mm displacements and those on the right are for ± 8 mm displacements; dots below force traces indicate stimulation times. Thin lines show measured forces and thick lines show forces predicted by the Hill model. Actual muscle forces were always lower than those predicted by the Hill model. (B) Summary data for the three animals in which these experiments were performed. Percent RMS errors between measured and modeled forces are plotted as a function of stimulation frequency for both perturbation amplitudes. Circles indicate actual data points. Open circles correspond to a different random length pattern tested in a single cat.

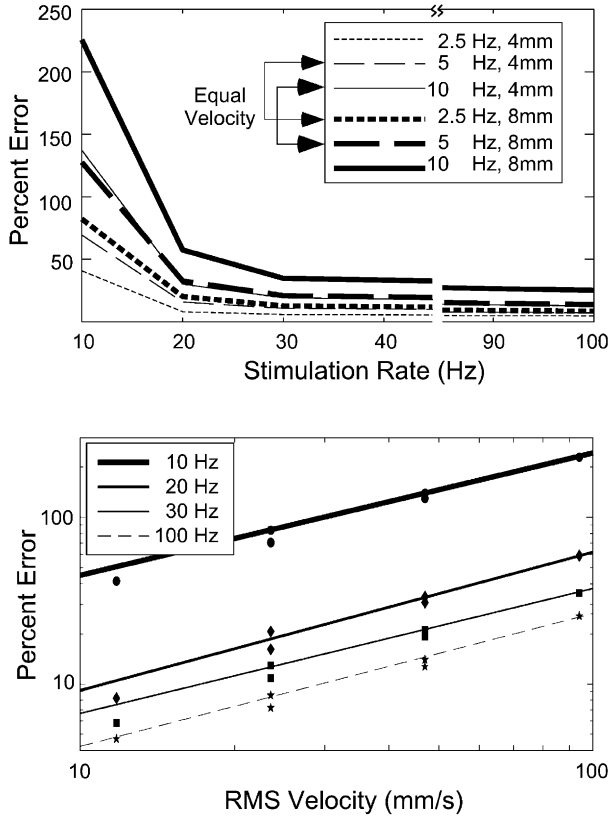

Fig. 3. Decreased Hill-model performance for larger perturbation amplitudes was due primarily to corresponding increases in muscle–tendon velocity. (A) Model errors as a function of stimulation rate for different combinations of perturbation bandwidth and amplitude. Lines connected by arrows have identical muscle velocities and different amplitudes. Data is for the single animal in which this expanded range of perturbation bandwidths and amplitudes was tested. (B) Model errors as a function of muscle velocity for each of the tested stimulation rates. Lines were fit using linear regression ($r^2 > 0.98$).

3. Results

During constant frequency electrical stimulation, Hill-model errors increased with decreasing stimulation rate and increasing perturbation amplitude (Fig. 2). These errors were manifested as a movement-related decrease in muscle force that was not accounted for by the Hill model. Results were consistent across the three cats used in this protocol, and did not vary with changes in the randomization of the length perturbation.

Decreased Hill-model performance with increased perturbation amplitude was associated primarily with increased muscle velocity, not increased muscle length (Fig. 3). To determine which of these factors was most important, a more complete set of perturbation bandwidths was tested in one animal. Bandwidth was varied by changing the displacement sequence output rate. Therefore, muscle velocity was proportional to the product of the bandwidth and amplitude. Trials with identical velocities had nearly identical Hill-model errors (Fig. 3A), even though displacement amplitudes differed. Note for example the errors associated with the 5 Hz, 8 mm trial and the 10 Hz, 4 mm trial. At each stimulation frequency, there was a nearly linear relationship ($r^2 > 0.98$) between the RMS muscle velocity and Hill-model error (Fig. 3B).

Hill-model errors for randomly stimulated muscle were similar to those obtained with constant stimulation for average stimulation rates of 20 Hz and 30 Hz, but errors at 10 Hz were substantially lower with random stimulation than with constant stimulation (Fig. 4). As with constant stimulation, errors were smaller for the

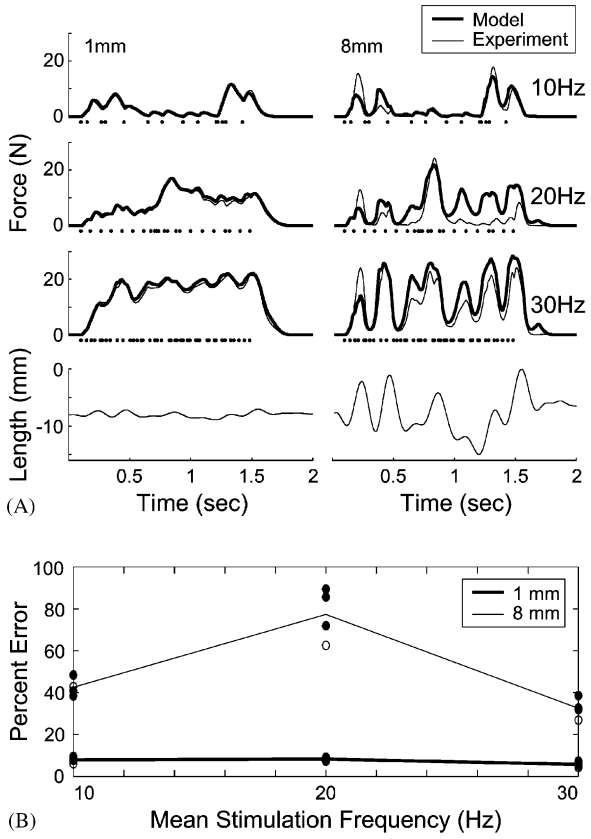

Fig. 4. Model errors with random stimulation IPIs were similar to those with continuous IPIs for average stimulation rates above 20 Hz. Figure format is identical to Fig. 2. (A) Typical data for one animal. (B) Summary data for all three animals in which this protocol was performed.

lower perturbation amplitudes. Again, these results were invariant with changes in the length and stimulation randomization. These results suggest that for stimulation rates above 20 Hz, Hill model performance is not critically dependent upon stimulation dynamics, but rather only mean stimulation rate.

The decreased Hill-model errors for the 10 Hz random stimulation relative to those for the 10 Hz continuous stimulation were due to improved model performance for IPIs less than 100 ms. An analysis of the IPIs contained in the 10 Hz random stimulation pattern showed that approximately 60% corresponded to instantaneous firing rates between 4 and 10 Hz and approximately 30% to rates above 20 Hz. To determine if this distribution could explain the relatively low model errors with 10 Hz random stimulation, we collected data in one animal using 5 Hz constant stimulation and a perturbation amplitude of ± 8 mm. Under these conditions, model errors were 43%, down from an average of 118% for the constant 10 Hz stimulation in this same animal. Hence, it appears that Hill-model errors peak in the vicinity of 10 Hz and decrease for both lower and higher stimulation rates. These results, coupled with the

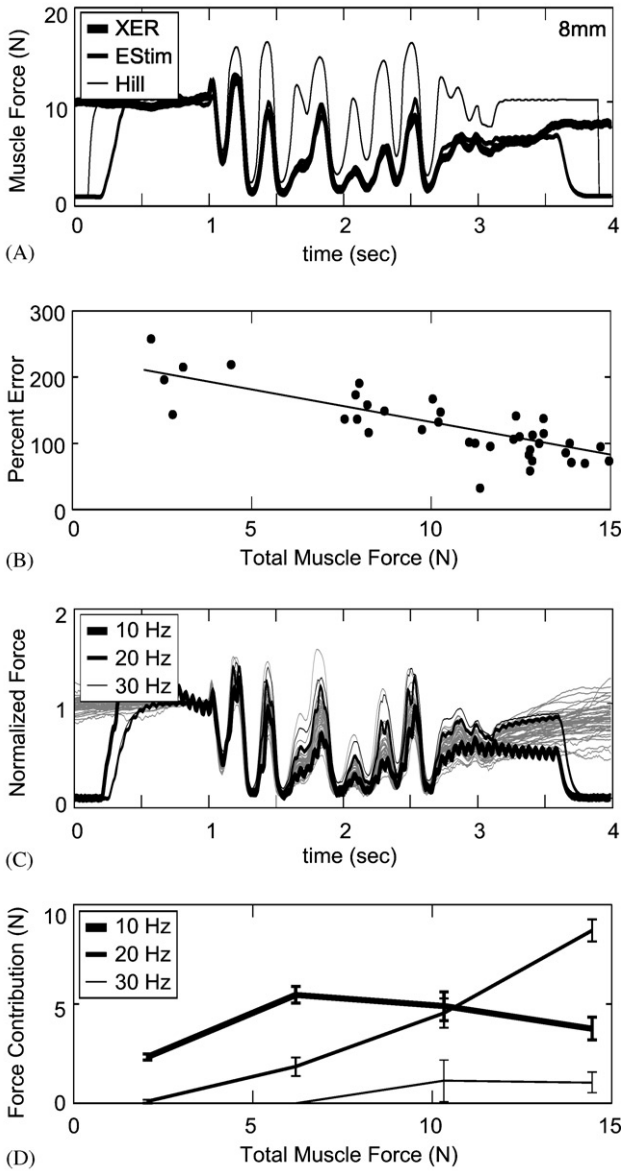

Fig. 5. Muscle force responses during natural activation most closely matched those obtained with 10–20 Hz constant frequency stimulation. (A) Typical force response to an applied perturbation (thick line) and the corresponding Hill-model prediction with a constant activation chosen to match the CXR force level before perturbation onset. The medium weight line shows the optimal combination of stimulation responses matched to this trial; the close match implies that CXR activation was nearly constant during this trial, indicating that variations in muscle activation did not contribute significantly to Hill-model errors. As with electrical stimulation, actual muscle forces were consistently less than those predicted by the Hill model. (B) Hill-model errors for one cat as a function of the pre-perturbation force level. (C) Force responses for the CXR trials (gray lines) normalized by the pre-perturbation force level and the corresponding normalized forces in response to constant electrical stimulation (black lines). (D) Estimated contributions of different motor unit firing rates to whole muscle force production. The force contributed by motor units firing at approximately 10, 20, and 30 Hz is plotted as a function of total muscle force. Computed from the same data presented in (B) and (C).

distribution of interspike intervals in the random stimulation patterns, explain the smaller errors for the 10 Hz random stimulation relative to the 10 Hz constant stimulation.

Hill-model errors for naturally activated muscle were most similar to the largest errors obtained during electrical stimulation. Again, actual muscle forces were consistently less than those predicted by the Hill model (Fig. 5A). Similar results were obtained from both cats in which the CXR was used to activate the soleus muscle. Percent RMS errors during movement decreased with increasing force level (Fig. 5B). At low forces, error magnitudes were comparable or higher than those obtained with 10 Hz constant stimulation. Errors decreased with increasing force level, but most remained above those measured at constant stimulation rates of 20 Hz and greater. Even though trials with large CXR activation changes were not analyzed, small fluctuations within the tolerance of our screening process may have added to the variability in the error force relationship.

One explanation for the large errors with CXR activation is that naturally recruited motor units fire predominantly in the 10–20 Hz range, where the errors to constant electrical stimulation were found to be greatest. This is supported by the normalized force responses obtained with CXR activation (Fig. 5C). Most crossed-extension responses lie between the normalized force responses for the 10 and 20 Hz constant stimulation rates. The actual firing rate distributions can be approximated using the optimization results used to select trials with steady activation by examining the weights chosen for each stimulation frequency (Fig. 5D). Over the forces tested, which were up to 80% of the maximum tetanic force in this animal, more than 85% of the total muscle force was contributed by motor units firing between approximately 10–20 Hz.

4. Discussion

This study evaluated Hill-muscle model accuracy during experimentally simulated functional conditions that included electrical activation at physiological rates and natural activation using the CXR. These activation paradigms were applied during continuous movements approximately matched to the length changes that occur during locomotion. Our results support the hypothesis that Hill-model errors during movement are greatest for the stimulation rates most relevant to normal movement conditions. For large muscle excursions, the errors for naturally activated muscle typically exceeded 50%, indicating that the Hill model is not appropriate for these conditions. Previous studies have reported substantially lower Hill-model errors ($\sim$10%) during movement, but have used only tetanic or near-tetanic stimulation (van Ingen Schenau et al., 1988; Sandercock and Heckman, 1997). Therefore, our current results underscore the importance of investigating more functionally relevant stimulation rates. These results were robust with respect to different length randomizations and stimulation patterns with variable IPIs, suggesting that our conclusions are general in nature.

The common Hill model simulated in this study assumes that muscle activation, force–velocity and length–tension properties are independent. This assumption is known to be incorrect. Activation depends on muscle length (Close, 1972; Stephenson and Wendt, 1984; Balnave and Allen, 1996), and also strongly influences length–tension and force–velocity properties (Joyce et al., 1969; Rack and Westbury, 1969; Roszek et al., 1994; Brown et al., 1999; Sandercock and Heckman, 2001). It is likely that these coupling effects led to the observed errors.

Length-related changes in calcium sensitivity result in length-dependent muscle activation (Close, 1972; Stephenson and Wendt, 1984; Balnave and Allen, 1996). This effect is greatest at low stimulation rates, when the response to intracellular calcium concentrations has not saturated. At lower rates, calcium sensitivity increases with muscle length, at least over the ascending limb of the tetanic length–tension curve. This length-dependent sensitivity may explain the shift in peak muscle force to longer lengths at lower stimulation rates (Rack and Westbury, 1969; Brown et al., 1999), and for naturally activated muscle (Sandercock and Heckman, 2001). Huijing has shown that stimulation dependent shifts in the length tension properties can lead to Hill-type model error predictions of up to 50% during isometric conditions (Huijing, 1998). These errors are similar to those reported in this study, and a similar mechanism may account for our results. However, during the dynamic conditions investigated in our experiments, Hill-model errors were related primarily to changes in muscle velocity, not length. Hence, strictly length-dependent changes in activation are not likely to account for our observations, although they may become more important in muscles with shorter fiber lengths and correspondingly steeper length–tension relations than the soleus.

The observed velocity-dependent errors were at least in part due to a movement-related decrease in muscle force that was not predicted by the Hill model. Similar velocity-dependent errors have been noted previously (Shue et al., 1995), as have decreases in mean force during continuous movement (Joyce et al., 1969; Kirsch et al., 1994). This movement-related force decrement is most prevalent at low stimulation rates, implying a coupling between activation and force-velocity properties. This phenomenon can be demonstrated in cross-bridge models incorporating a dependence between

physiologically based activation and cross-bridge attachment (Zahalak and Ma, 1990). It may also be facilitated by movement-enhanced calcium release from troponin, which can accelerate muscle relaxation (Caputo et al., 1994), or by a movement-related decreased in cooperativity between neighboring actin–myosin force generating sites (Gordon et al., 2000).

Two recent studies have attempted to modify the Hill model to account for the errors associated with assuming an invariant normalized force–velocity relationship. Shue et al. (1995, 1998) implemented a direct coupling between activation, length and velocity. Brown et al. (1999, 2000) coupled activation to a delayed version of muscle length, a method that indirectly allowed their model to replicate some of the known interactions between muscle velocity and activation. Both methodologies improved model performance over a range of experimental conditions, indicating that better representation of these interactions is key to improving Hill-model performance. Our results emphasize the importance of such modifications if Hill-type models are to be used for naturally activated muscle.

Acknowledgements

This work was supported by NIH grants NIAMS-AR41531 and 5-T32-HD07418, and a National Science Foundation grant awarded in 2001 to EJP.

References

Balnave, C.D., Allen, D.G., 1996. The effect of muscle length on intracellular calcium and force in single fibres from mouse skeletal muscle. Journal of Physiology (London) 492, 705–713.

Brown, I.E., Loeb, G.E., 2000. Measured and modeled properties of mammalian skeletal muscle: IV. Dynamics of activation and deactivation. Journal of Muscle Research and Cell Motility 21, 33–47.

Brown, I.E., Scott, S.H., Loeb, G.E., 1996. Mechanics of feline soleus: II. Design and validation of a mathematical model. Journal of Muscle Research and Cell Motility 17, 221–233.

Brown, I.E., Cheng, E.J., Loeb, G.E., 1999. Measured and modeled properties of mammalian skeletal muscle. II. The effects of stimulus frequency on force–length and force–velocity relationships. Journal of Muscle Research and Cell Motility 20, 627–643.

Burke, R.E., Levine, D.N., Salcman, M., Tsairis, P., 1974. Motor units in cat soleus muscle: physiological, histochemical and morphological characteristics. Journal of Physiology (London) 238, 503–514.

Caputo, C., Edman, K.A., Lou, F., Sun, Y.B., 1994. Variation in myoplasmic Ca_2+ concentration during contraction and relaxation studied by the indicator fluo-3 in frog muscle fibres. Journal of Physiology 478, 137–148.

Close, R.I., 1972. The relations between sarcomere length and characteristics of isometric twitch contractions of frog sartorius muscle. Journal of Physiology 220, 745–762.

Cordo, P.J., Rymer, W.Z., 1982. Motor-unit activation patterns in lengthening and isometric contractions of hindlimb extensor muscles in the decerebrate cat. Journal of Neurophysiology 47, 782–796.

Edman, K.A., Caputo, C., Lou, F., 1993. Depression of tetanic force induced by loaded shortening of frog muscle fibres. Journal of Physiology (London) 466, 535–552.

Gerritsen, K.G., Nachbauer, W., van den Bogert, A.J., 1996. Computer simulation of landing movement in downhill skiing: anterior cruciate ligament injuries. Journal of Biomechanics 29, 845–854.

Gordon, A.M., Homsher, E., Regnier, M., 2000. Regulation of contraction in striated muscle. Physiological Review 80, 853–924.

Goslow Jr., G.E., Reinking, R.M., Stuart, D.G., 1973. The cat step cycle: hind limb joint angles and muscle lengths during unrestrained locomotion. Journal of Morphology 141, 1–41.

Huijing, P.A., 1998. Muscle, the motor of movement: properties in function, experiment and modelling. Journal of Electromyography and Kinesiology 8, 61–77.

Jewell, B.R., Wilkie, D.R., 1960. The mechanical properties of relaxing muscle. Journal of Physiology (London) 152, 30–47.

Joyce, G.C., Rack, P.M., Westbury, D.R., 1969. The mechanical properties of cat soleus muscle during controlled lengthening and shortening movements. Journal of Physiology 204, 461–474.

Kirsch, R.F., Boskov, D., Rymer, W.Z., 1994. Muscle stiffness during transient and continuous movements of cat muscle: perturbation characteristics and physiological relevance. IEEE Transactions on Biomedical Engineering 41, 758–770.

Meijer, K., Grootenboer, H.J., Koopman, H.F., van der Linden, B.J., Huijing, P.A., 1998. A hill type model of rat medial gastrocnemius muscle that accounts for shortening history effects. Journal of Biomechanics 31, 555–563.

Morgan, D.L., 1994. An explanation for residual increased tension in striated muscle after stretch during contraction. Experimental Physiology 79, 831–838.

Nichols, T.R., Houk, J.C., 1976. Improvement in linearity and regulation of stiffness that results from actions of stretch reflex. Journal of Neurophysiology 39, 119–142.

Powers, R.K., Rymer, W.Z., 1988. Effects of acute dorsal spinal hemisection on motoneuron discharge in the medial gastrocnemius of the decerebrate cat. Journal of Neurophysiology 59, 1540–1556.

Press, W., Flannery, B.P., Teukolsky, S.A., Vetterling, W.T., 1986. Numerical Recipes. Cambridge University Press, New York.

Rack, P.M.H., Westbury, D.R., 1969. The effects of length and stimulus rate on tension in the isometric cat soleus muscle. Journal of Physiology 204, 443–460.

Roszek, B., Baan, G.C., Huijing, P.A., 1994. Decreasing stimulation frequency-dependent length–force characteristics of rat muscle. Journal of Applied Physiology 77, 2115–2124.

Sandercock, T.G., Heckman, C.J., 1997. Force from cat soleus muscle during imposed locomotor-like movements: experimental data versus Hill-type model predictions. Journal of Neurophysiology 77, 1538–1552.

Sandercock, T.G., Heckman, C.J., 2001. Whole muscle length–tension properties vary with recruitment and rate modulation in a reflexive cat soleus. Journal of Neurophysiology 85, 1033–1038.

Shue, G.H., Crago, P.E., 1998. Muscle–tendon model with length history-dependent activation–velocity coupling. Annals of Biomedical Engineering 26, 369–380.

Shue, G., Crago, P.E., Chizeck, H.J., 1995. Muscle–joint models incorporating activation dynamics, moment-angle, and moment-velocity properties. IEEE Transactions on Biomedical Engineering 42, 212–223.

Stephenson, D.G., Wendt, I.R., 1984. Length dependence of changes in sarcoplasmic calcium concentration and myofibrillar calcium

sensitivity in striated muscle fibres. Journal of Muscle Research and Cell Motility 5, 243–272.

van der Helm, F.C.T., 2000. Large-scale musculoskeletal systems: sensorimotor integration and optimization. In: Winters, J.M., Crago, P.E. (Eds.), Biomechanics and Neural Control of Posture and Movement. Springer, New York, pp. 407–424.

van Ingen Schenau, G.J., Bobbert, M.F., Ettema, G.J., de Graaf, J.B., Huijing, P.A., 1988. A simulation of rat edl force output based on intrinsic muscle properties. Journal of Biomechanics 21, 815–824.

Winters, J.M., 1990. Hill-based muscle models: a systems engineering perspective. In: Winters, J.M., Woo, S.L. (Eds.), Multiple Muscle Systems: Biomechanics and Movement Organization. Springer, New York, pp. 69–93.

Zahalak, G.I., 1986. A comparison of the mechanical behavior of the cat soleus muscle with a distribution-moment model. Journal of Biomechanical Engineering 108, 131–140.

Zahalak, G.I., Ma, S.P., 1990. Muscle activation and contraction: constitutive relations based directly on cross-bridge kinetics. Journal of Biomechanical Engineering 112, 52–62.

Zajac, F.E., 1989. Muscle and tendon: properties, models, scaling, and application to biomechanics and motor control. Critical Reviews in Biomedical Engineering 17, 359–411.